Band Gap Improvement in Hollow-Core Photonic Crystal Fiber

[1]LEBBAL MOHAMED REDHA, [2]SALIM GHALEM, [3]AHLEM BENMERKHI, [4]BOUCHEMAT TOURAYA, [5]BOUCHEMAT MOHAMED
[1, 2, 3, 4, 5] Department of Electronics, Laboratory L.M.I., University of Constantine 1, Constantine, ALGERIA

Email: [1]lebbalmohamedredha@yahoo.fr, [2]salimghalem2015@gmail.com, [3]ahlemelec@hotmail.fr, [4]tboumaza2001@yahoo.fr , [5]hm_bouchemat@yahoo.fr,

Abstract: - In this paper, due to a negligible contribution from the core material (air) we investigate the band gap width in a photonic crystal fiber with hollow core, the fiber is based on silica or silicon. Simulation results shows a dependence between the band width and the filling factor, also we can notice that the band width in a fiber with square lattice is higher than the hexagonal lattice structure. Also, we have study of the band gap according to the filling of the rings and we notice that we can increase the band gap width by filling the second holes ring close to the guiding core fiber by silicon.

Key words: -Band gap, Fiber, Filling Factor, propagation constant, Silica, Silicone, Holes Arrays.

1 Introduction

Photonic crystal fibers (PCFs), have attracted much research attention and has been appointed as one of the most intriguing structures for various optical applications [1-5]. These fibers can be divided by the guidance type into two categories: effective index guidance [6-8] and photonic-band-gap (PBG) guidance [9-11]. The first type of fiber the light is guiding in the central defect with high index region. This allows the light to be guided by total internal reflection (TIR). In this work we study the second type of PCFs which based on the PBG and have the capability to control the guidance of light within a certain frequency band, light is confined in a low-index core by reflection from a photonic crystal cladding.

The study of photonic crystals and their specific properties, naturally leads to the study of the behavior of light in photonic band gap materials [12-14]. The manufacturing technology of PCFs allows the tuning of the optical properties by changing the size, shape and position of the cladding holes.

So several studies have been reported to improve the band gap width of PBG guidance fibers to increase the band transmission frequency.

For that in this work we study the band gap as a function of the propagation constant of modes, the based material and the filling factor for a hexagonal and square lattice holes[15-17] finally the influence of the filling holes of rings [18,19] to the band gap width.

2 Fiber hexagonal structure

2.1. Study of the band gap as a function of the propagation constant

Fig.1 shows the index profile of a photonic band gap-guided fiber with hexagonal *air holes* arrays.

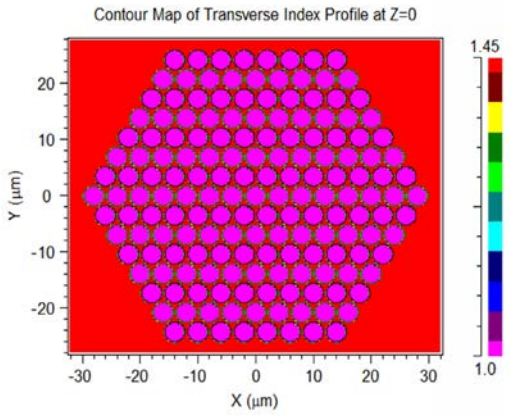

Figure 1. Photonic crystal fiber with hexagonal air holes arrays

The index profile shown in Fig.1 is calculated for the plane z = 0, it is a periodic air holes arrays (index n = 1) in a material based on Silicon (nSiO2 = 1.45). The light will be guided into the central air hole.
Fig.2 and Fig.3 represent the diagrams of the bands calculated for a hexagonal 2D lattice characterized

by a filling factor 0.7, a propagation constant β and a period Λ. As a light source, we use a plane wave of the Gaussian type. One of the main results of these figures relates to the difference in behavior between the electric transverse TE, the magnetic transverse TM and the hybrid polarizations.

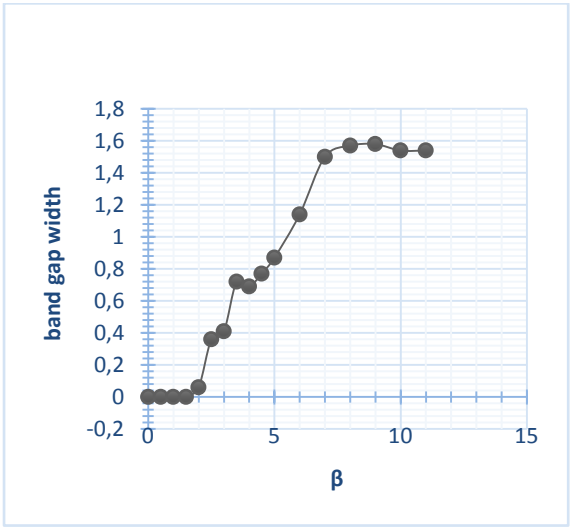

Figure 2. Variation of the band width for the silica/air hexagonal lattice versus the propagation constant β(μm^{-1}).

For the propagation constant null for silica-air lattices there is no gaps in either TE or TM polarization. But in fig.2, silica-air lattices can support bands gaps for propagation out of the plane in hybrid polarization.

(a)

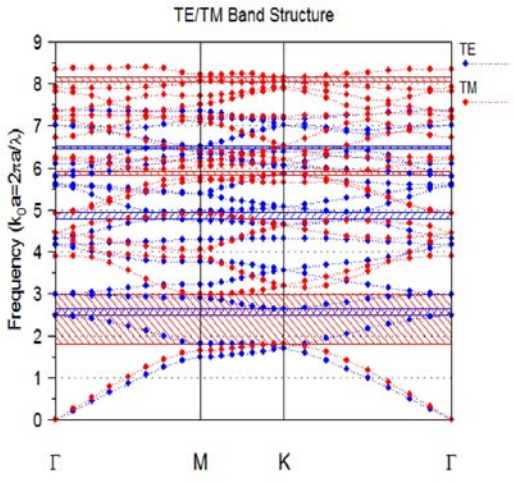

(b)

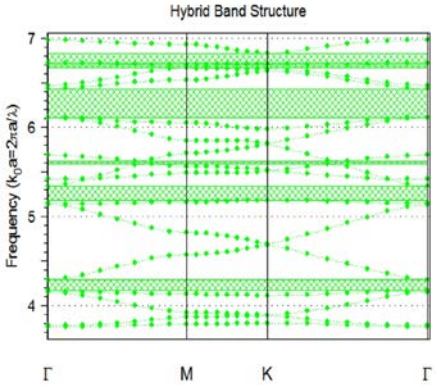

Figure 3. Band structures for the periodic air holes in silicon hexagonal lattice of fiber (a) for β=0 and (b) for β = 2.25 μm^{-1} with n=3.42

By comparison in Fig.2 and Fig.3, it is noted that if the index contrast between the matrix of the based material and the air holes is increased, the width of the spectral band increases in the plane of the fiber for β = 0 or out of plane when β is different from 0.

2.2 Study of the band gap width as a function of the based material and the filling factor of holes.

For the study of the band gap, simulations were made for different holes filling factors and for different materials.

1st case: for a silica based material and refraction index n=1.45.

(a)

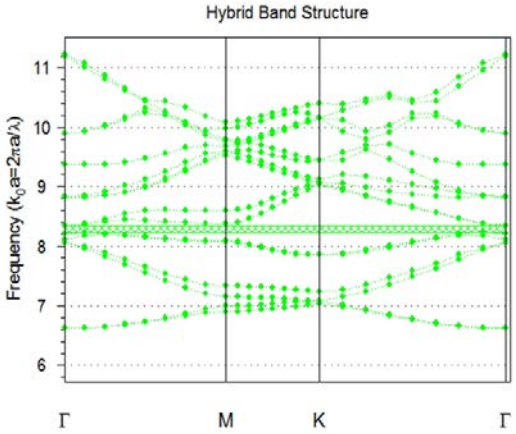

(b)

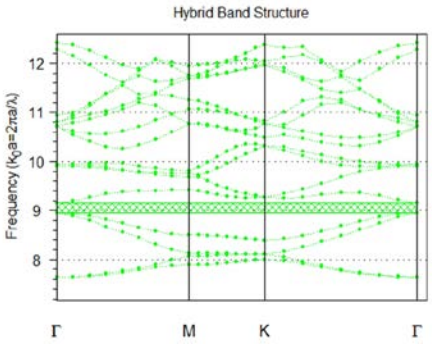

(c)

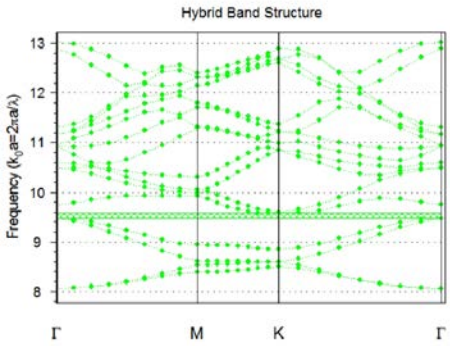

(d)

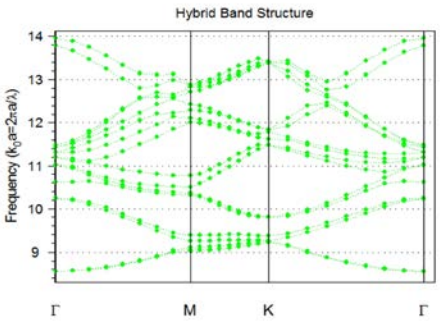

Figure 4. Band structures for the silica/air hexagonal lattice as a function of the filling factor of holes *f* (a) for *f*=0.3 (b) for *f*=0.7 (c) for *f*=0.8 (d) for *f* =0.9

Fig.4 shows the band diagrams versus the different filling factors (*f*) for a silica/air hexagonal lattice, based on these results, Fig.5 shows the filling factor variation curve as a function of the width of the spectral band.

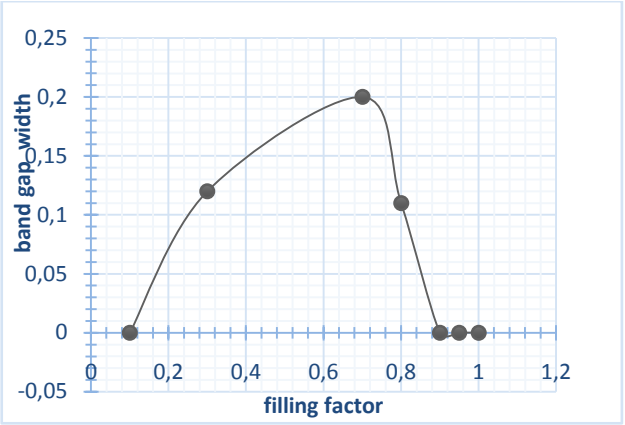

Figure 5. Spectral band width variation as a function of the filling factor for a silica/air hexagonal lattice.

It can be seen from Fig.5, that the spectral band increases as a function of the filling factor increasing when $f \leq 0.7$, after this value, even if the filling factor value is increased, the spectral band decreases for $0.7 < f \leq 0.9$ and the band becomes null after that.

2nd case: for a silicon based material and refraction index n = 3.42

(a)

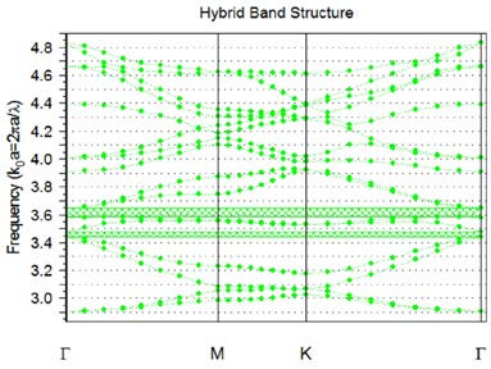

(b)

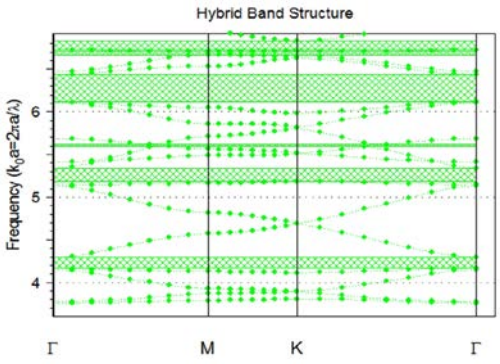

(c)

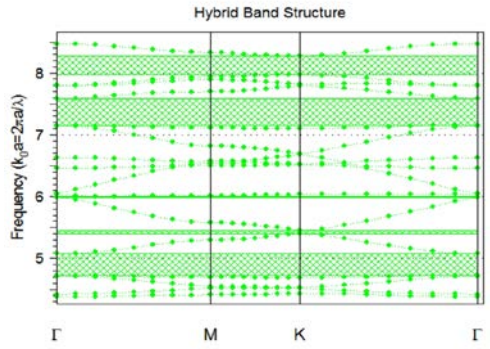

(d)

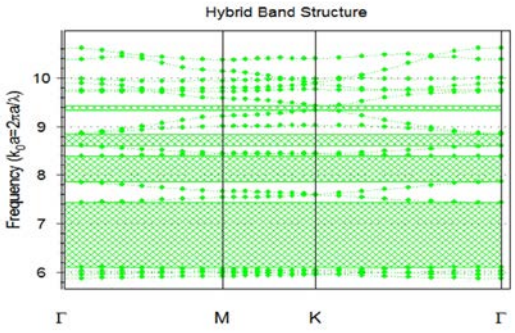

Figure 6. Band structures for the silicon/air hexagonal lattice as a function of the holes filling factor *f* for (a) *f*=0.3 (b) *f*=0.7 (c) *f*=0.8 (d) *f*=0.9

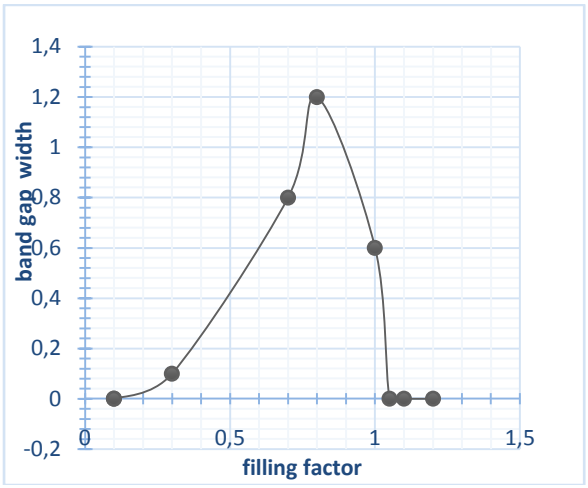

Figure 7. Spectral band width variation as a function of the filling factor for a silicon/air hexagonal lattice.

It can be seen from Fig.7 that in each case the value of the filling factor is increased, the spectral band increases to the maximum when $f \leq 0.9$, after this value the spectral band decreases for $0.9 < f \leq 1.04$ and the band becomes null after that.

It can also be seen from Fig.7 and Fig.5 that if the contrast of index is increased in a fiber the width of the band gap increases also. Thus, the contrast of index is proportional to the band gap width increasing.

3 Fiber square structure

3.1 Study of the band gap as a function of the propagation constant

The index profile of the photonic fiber based on silica/air square lattice is shown in Fig.8

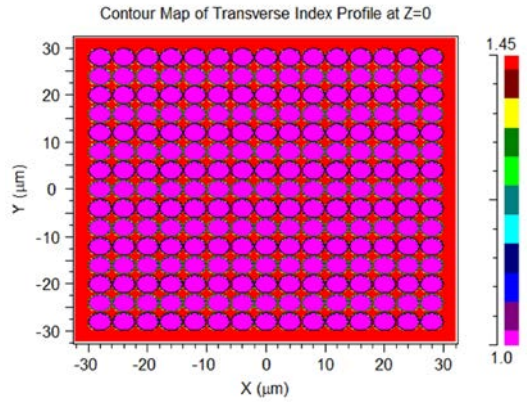

Figure 8. Photonic crystal fiber with square air holes arrays

The index profile shown in Fig.8 is calculated for the plane z = 0, it is a periodic square lattice of air holes (index n = 1) in silica ($n_{SiO2} = 1.45$). The light will be guided into the central air hole.
Fig.9 and Fig.10 represent the diagrams of the bands for the silica/air square lattice characterized by a filling factor, a propagation constant β and a period Λ.The results of these figures relates to the difference in behavior between the electric transverse TE, the magnetic transverse TM and the hybrid polarizations is shown in this section.

(a)

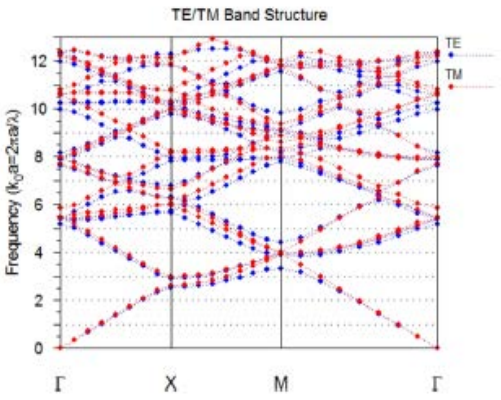

(b)

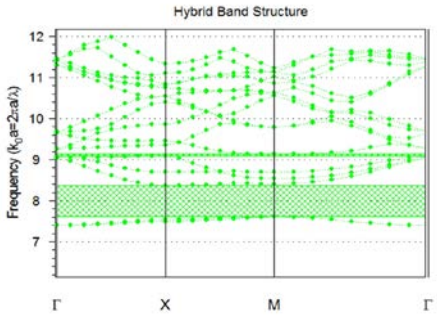

Figure 9. Band structures for the silica/air square lattice (a) for β=0 and (b) for β = 2.25 μm^{-1}

By comparison between Fig.9 and Fig.2, if the lattice of holes is changed for the same characteristics of the fiber Fig.9 (a and b), the width of the spectral band increases out of plane (for β different from 0) but for β=0 in the plane of fiber always for low contrast (silica/air) and for both types of lattices it is found that there are no bands gaps.

3.2 Study of the band gap width as a function of the based material and the filling factor of holes.

To study the band gap of fibers based on a square lattice as a function of the holes filling factors, simulations were performed for different filling factor values

(a)

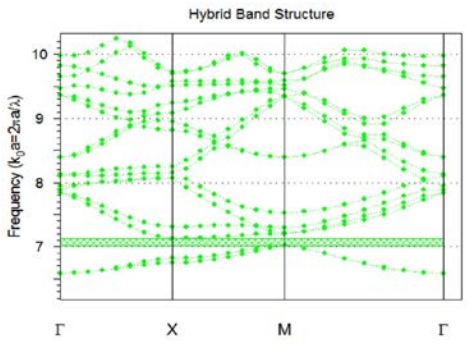

(b)

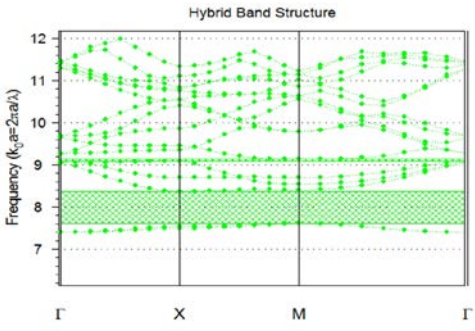

(c)

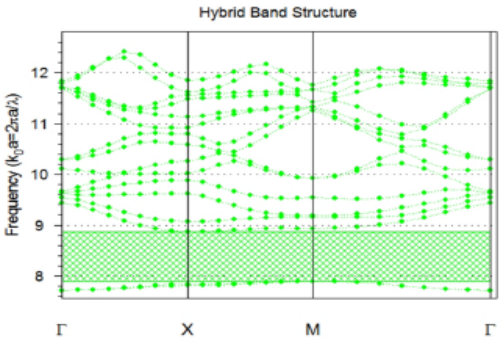

(d)

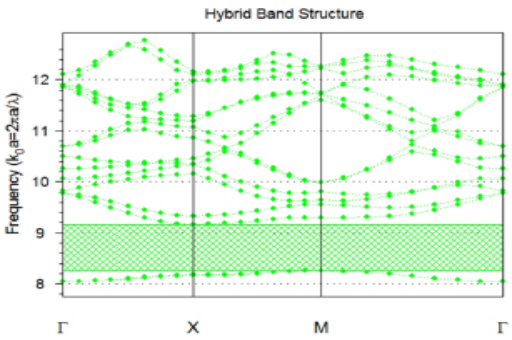

Figure 10. Band structures for the silica/air hexagonal lattice as a function of the filling factor of holes *f* (a) for *f*=0.3 (b) for *f*=0.7 (c) for *f*=0.8 (d) for *f* =0.9

Fig.10 shows the band diagrams for different filling factors (*f*) for a silica/air square lattice, based on these results, Fig.11 shows the filling factor variation curve as a function of the width of the spectral band.

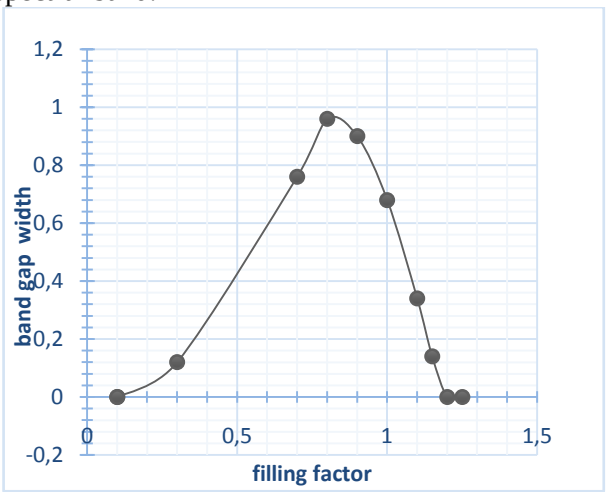

Figure 11. Spectral band width variation as a function of the filling factor for a silica/air square lattice.

It can be seen from Fig.11 if the filling factor increases from 0 to 0.8, the spectral band increases proportional to the filling factor increasing, after that even if the filling factor value is increased the spectral band gap decreases and become null for *f=1.2*.
It can be concluded from this results that if the index contrast is increased in a fiber, the spectral band increases even in the plane of the fiber. This variation makes it possible to increase the number of guided waves in the fiber based on the photonic band gap guidance.
Also the variation of the spectral band for the square lattice structure is better than the hexagonal structure for the same filling factor value.
Thus, the ratio of the high and low index surfaces and the filling factor in a photonic crystal fiber are determining factors for the bands gaps width.

4 Study of the band gap width as a function of the rings filling

In this section, the band gap is studied as a function of the rings filling, for different steps the rings of different lines of fiber (ring 1, 2, 3 and 4) are filled with the silicon ($n_{Si} = 3.42$).

1st case: filling the first ring by silicon

(a)

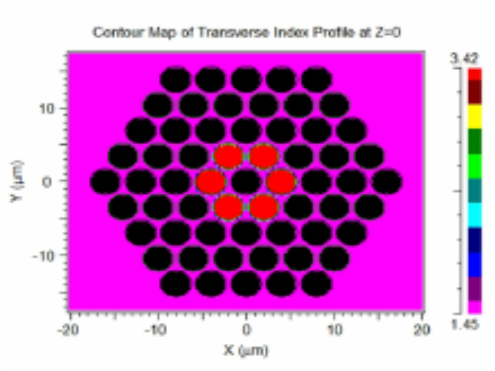

(b)

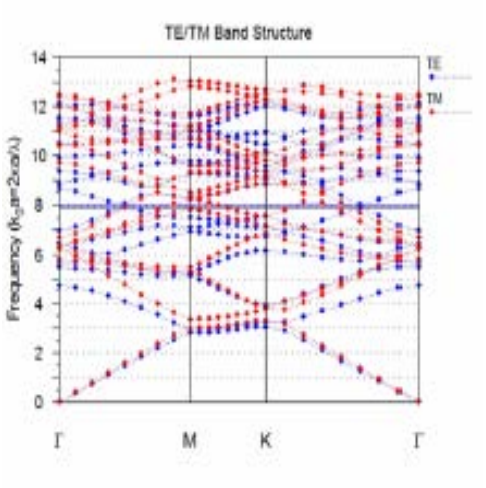

(c)

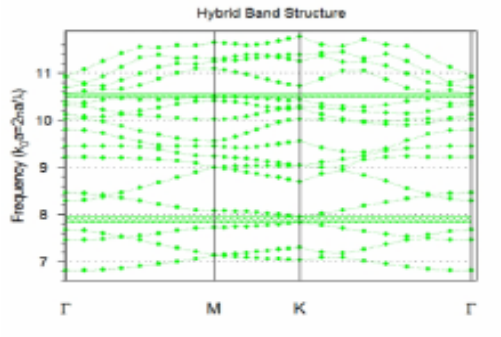

Figure 12. (a) Photonic crystal fiber with silica/air hexagonal air holes arrays and filling the first ring by silicon, (b) band diagram for β = 0, and (c) for β =9/Λ.

2nd case: filling the second ring by silicon

(a)

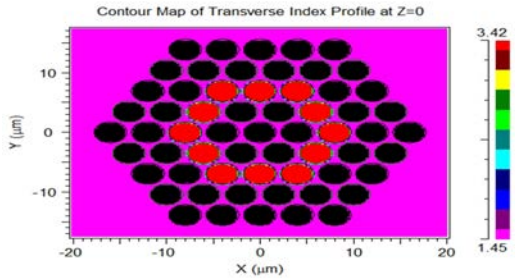

(b)

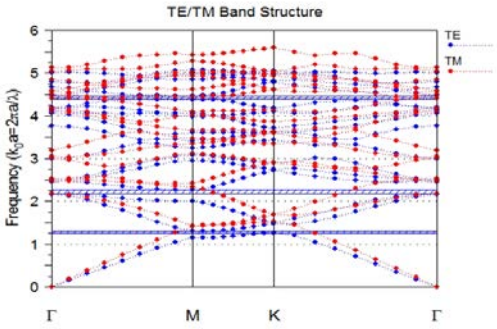

(c)

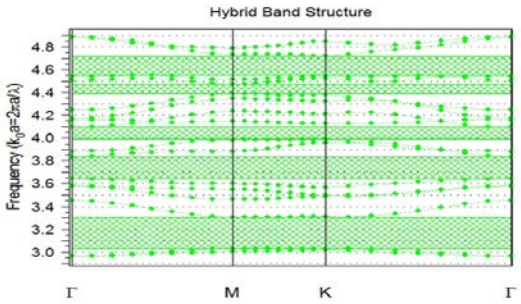

Figure 13. (a) Photonic crystal fiber with silica/air hexagonal air holes arrays and filling the second ring by silicon, (b) band diagram for β = 0, and (c) for β=9/*Λ*.

3rd case: filling the third ring by silicon

(a)

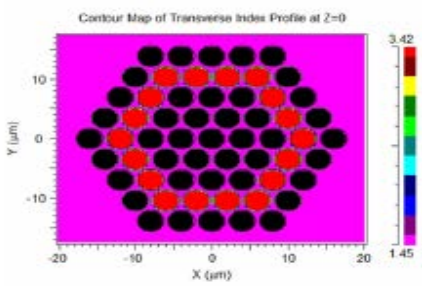

(b)

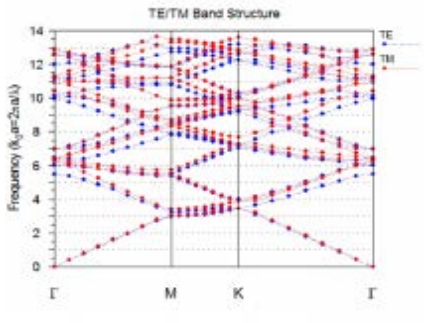

(c)

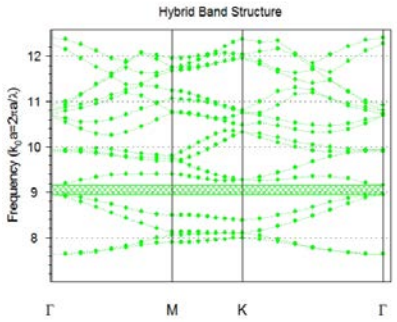

Figure 14. (a) Photonic crystal fiber with silica/air hexagonal air holes arrays and filling the third ring by silicon, (b) band diagram for β = 0, and (c) for β =9/*Λ*.

4th case: filling the fourth ring by silicon

(a)

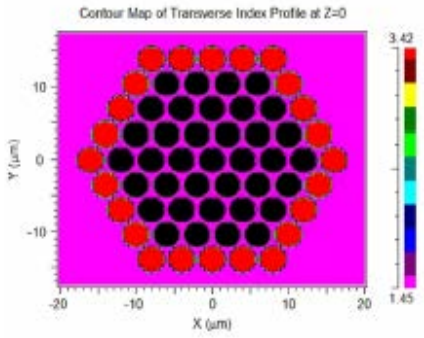

(b)

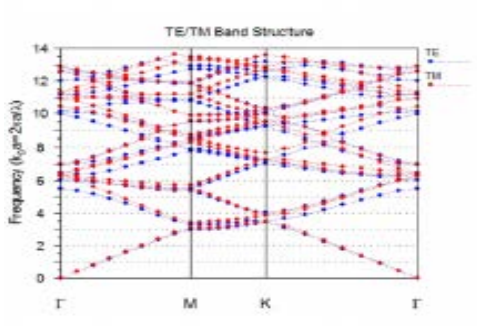

(c)

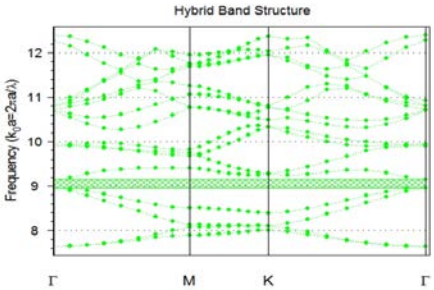

Figure 15. (a) Photonic crystal fiber with silica/air hexagonal air holes arrays and filling the fourth ring

by silicon, (b) band diagram for $\beta = 0$, and (c) for $\beta=9/\Lambda$.

It is observed from this study, which represents the band gap width variation as a function of the rings filling in the plane of the fiber and out of plane, if the first or the second ring is filled with silicon the band gap width increases for in or out of plane as a function of the number of filled holes (first ring with 6 holes and 12 for the second ring) ; but if the filled holes distance is further from the core (the third and fourth ring), the behavior of the band gap diagram become as if the holes has not been filled with silicon.

5 Conclusion

The dependencies of photonic band gap PBG of photonic crystal fiber, the air holes lattice, the filling factor and the filled holes by silicone have been theoretically studied. The different PBG open for TE and TM and Hybrid modes is determined for various values of these three important parameters. Furthermore, we have optimized parameters of the fiber to achieve wider PBG which is useful for guiding light in very large spectral band and decreasing propagation losses.

References:

[1] Guillermo A. Cárdenas-Sevilla, Vittoria Finazzi, Joel Villatoro, Valerio Pruneri “Photonic crystal fiber sensor array based on modes overlapping.” 11 April 2011 / Vol. 19, No. 8 / OPTICS EXPRESS.

[2] D. Vigneswaran, N. Ayyanar, Mohit Sharma, M. Sumathi, M.S.Mani Rajan, K.Porsezian “Salinity sensor using photonic crystal fiber” Sensors and Actuators A: Physical, volume 269, 1 January 2018, Pages 22-28.

[3] Jianqun Cheng, Jianrong Qiu, Shuangchen Ruan “Switchable quadruple-wavelength erbium-doped photonic crystal fiber laser based on a polarization-maintaining photonic crystal fiber Sagnac loop filter” Optics & Laser Technology, volume 58, June 2014, Pages 110-113.

[4] Guowen An, Shuguang Li, Yinghong An, Haiyang Wang, Xuenan Zhang “Glucose sensor realized with photonic crystal fiber-based Sagnac interferometer” Optics Communications, Volume 405, 15 December 2017, Pages 143-146.

[5] G.S.B. Filho, D.G. Correia, W.B. de Fraga, G.F. Guimarães “Obtaining optical logic gates – OR, XOR, AND and logic functions using asymmetric Mach-Zehnder interferometer based on photonic crystal fiber” Optics & Laser Technology, Volume 97, 1 December 2017, Pages 370-378.

[6] M.R. Lebbal, T. Boumaza, M. Bouchemat “Structural study of the single-mode photonic crystal fiber ”, Optik - Int. J. Light Electron Opt. (2013)

[7] Laleh Mousavi, Mohammad Sabaeian, Hamid Nadgaran “Thermally-induced birefringence in solid-core photonic crystal fiber lasers” Optics Communications, Volume 300, 15 July 2013, Pages 69-76.

[8] Vinay Kanungo, Sanjeev Kumar Metya, Vijay Janyani, Mohammad Salim “Segmented cladding index guiding photonic crystal fiber” Optics Communications, Volume 297, 15 June 2013, Pages 147-153.

[9] Z.Q.Zhao, Y.Lu, L.C.Duan, M.T.Wang, H.W.Zhang, J.Q.Yao “Fiber ring laser sensor based on hollow-core photonic crystal fiber” Optics Communications, Volume 350, 1 September 2015, Pages 296-300.

[10] Zoltán Várallyay, Péter Kovács “All-silica, large mode area, single mode photonic bandgap fibre with Fabry–Perot resonant structures” Optical Fiber Technology, Volume 28, March 2016, Pages 1-6.

[11] S. Arismar Cerqueira, A.R. do Nascimento, I.A.M. Bonomini, M.A.R. Franco, V.A.Serrão, C.M.B. Cordeiro “Strong power transfer between photonic bandgaps of hybrid photonic crystal fibers” Optical Fiber Technology, Volume 22, March 2015, Pages 36-41.

[12] Arun Kumar, Vipin Kumar, Anuradha Nautiyal, Kh. S. Singh, S.P. Ojha “Optical switch based on nonlinear one dimensional photonic band gap material” Optik - International Journal for Light and Electron Optics, Volume 145, September 2017, Pages 473-478.

[13] A. EL Haddad “Exact analytical solution for the electromagnetic wave propagation in a photonic band gaps material with sinusoidal periodicity of dielectric permittivity” Optik - International Journal for Light and Electron Optics, Volume 127, Issue 4, February 2016, Pages 1627-1629.

[14] Rathinam Balamurugan, Jui-Hsiang Liu “A review of the fabrication of photonic band gap materials based on cholesteric liquid crystals”

Reactive and Functional Polymers, Volume 105, August 2016, Pages 9-34.

[15] Yoshiki Nakata, Masataka Yoshida, Kazuhito Osawa, Noriaki Miyanaga "Fabricating a regular hexagonal lattice structure by interference pattern of six femtosecond laser beams" Applied Surface Science, Volume 417, 30 September 2017, Pages 69-72.

[16] Dinesh Kumar Sharma, Anurag Sharma, Saurabh Mani Tripathi "Characteristics of solid-core square-lattice microstructured optical fibers using an analytical field model" Optics & Laser Technology, Volume 96, 1 November 2017, Pages 97-106.

[17] Shahram Moradi, Alperen Govdeli, Serdar Kocaman "Zero average index design via perturbation of hexagonal photonic crystal lattice" Optical Materials, Volume 73, November 2017, Pages 577-584.

[18] Mona Kalantari, Arash Karimkhani, Hamed Saghaei "Ultra-Wide mid-IR supercontinuum generation in As2S3 photonic crystal fiber by rods filling technique" Optik - International Journal for Light and Electron Optics, Volume 158, April 2018, Pages 142-151.

[19] Ali Dideban, Hamidreza Habibiyan, Hassan Ghafoorifard "Photonic crystal channel drop filter based on ring-shaped defects for DWDM systems" Physica E: Low-dimensional Systems and Nanostructures, Volume 87, March 2017, Pages 77-83.